APPLIED ORGANOMETALLIC CHEMISTRY
Appl. Organometal. Chem. 2006; **20**: 203–213
Materials, Nanoscience and Catalysis AOC
Published online 12 December 2005 in Wiley InterScience (www.interscience.wiley.com). DOI:10.1002/aoc.1026

Preparation, spectral characterization, electrochemistry, EXAFS, antibacterial and catalytic activity of new ruthenium (III) complexes containing ONS donor ligands with triphenylphosphine/arsine

R. Prabhakaran[1], V. Krishnan[2], K. Pasumpon[3], D. Sukanya[1], E. Wendel[2], C. Jayabalakrishnan[3], H. Bertagnolli[2] and K. Natarajan[1]*

[1]Department of Chemistry, Bharathiar University, Coimbatore 641046, India
[2]Institute of Physical Chemistry, University of Stuttgart, Pfaffenwaldring 55, 70569, Stuttgart, Germany
[3]Sri Ramakrishna Mission Vidyalaya College of Arts and Science, Coimbatore 641020, India

Received 31 August 2005; Revised 17 October 2005; Accepted 25 October 2005

New hexa-coordinated ruthenium (III) complexes of the type $[RuX(EPh_3)_2(L)]$ (X = Cl or Br; L = dibasic tridentate Schiff base ligand; E = P or As) have been synthesized by the reactions of $[RuCl_3(PPh_3)_3]$, $[RuCl_3(AsPh_3)_3]$ or $[RuBr_3(AsPh_3)_3]$ with the appropriate Schiff base ligands derived by the condensation of salicylaldehyde and 2-hydroxy-1-naphthaldehyde with N(4) substituted thiosemicarbazones. All the new complexes were characterized using various physico-chemical methods such as elemental analyses, infrared, electron paramagnetic resonance (EPR) spectroscopy, magnetic moment and cyclic voltammetry. Based on the extended X-ray absorption fine structure (EXAFS) analysis, an octahedral structure has been confirmed for the complexes. The new complexes have been subjected to the catalytic activity and antibacterial studies. Copyright © 2005 John Wiley & Sons, Ltd.

KEYWORDS: ruthenium complexes; EPR; cyclic voltammetry; EXAFS; catalytic activity

INTRODUCTION

The choice of ligands which forces metal ions into unusual geometries that stabilize specific oxidation states is of interest in the development of a catalytic system relevant to bioinorganic chemistry. A large number of reports have appeared not only in the area of preparation of efficient catalysts, but also in developing agents for defence mechanisms against microorganisms and tumours.[1–8] In this area of research semicarbazones and thiosemicarbazones containing nitrogen and oxygen/sulfur donor ligands have been widely studied. Thiosemicarbazones and their transition metal complexes have been extensively studied in recent years owing to their pharmacological properties.[9–12] Schiff base ligands have been extensively investigated with regard to their numerous applications in organic synthesis as well as in pharmacology. The planarity of the ligand provides a means of creating a large vacant site, where coordination of a transition metal could be carried out. Tridentate Schiff base ligands have been successfully used in several catalytic asymmetric reactions.[13,14] The influence of triphenylphosphine/arsine in the catalytic reaction cycle has also been examined extensively.[15–19] Several ruthenium (II) and ruthenium (III) complexes are of importance not only because of their use in catalytic reactions like oxidation[20–25] and hydrogenation,[26–29] but also due to their medicinal properties.[30–32] In connection with our ongoing interest in this field of research, we have already investigated several ruthenium (II) and ruthenium (III) complexes.[33–37]

In view of the growing interest in the biological and catalytic activities of ruthenium complexes, we intend to develop a single compound effective for both biological and catalytic studies. In this article, we report the preparation, catalytic activity and antibacterial properties of a series of new ruthenium (III) thiosemicarbazone complexes with triphenylphosphine/arsine. The complexes of this type are

*Correspondence to: K. Natarajan, Department of Chemistry, Bharathiar University, Coimbatore 641046, India.
E-mail: k_natraj6@yahoo.com

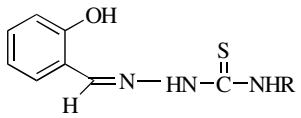

Salicylaldehyde-N-phenylthiosemicarbazide (Sal-Nptsc), R = C_6H_5

Salicylaldehyde-N-methylthiosemicarbazide (Sal-Nmtsc), R = CH_3

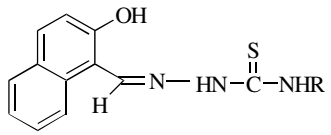

Napthaldehyde-N-phenylthiosemicarbazide (Nap-Nptsc), R = C_6H_5

Napthaldehyde N-methylthiosemicarbazide (Nap-Nmtsc), R = CH_3

Figure 1. General structure of the Schiff base ligands.

expected to exhibit biological activity as well as catalytic activity due to the presence of both thiosemicarbazone and triphenylphosphine/arsine moieties. These complexes are characterized by extended X-ray absorption fine structure (EXAFS), infrared (IR), electron paramagnetic resonance (EPR) spectroscopy and cyclic voltammetry. The general structure of the ligands used in the present work is shown in Fig. 1.

EXPERIMENTAL

Materials

All the reagents used were chemically pure or analytical reagent grade. Solvents were purified and dried according to standard procedures.[38] $RuCl_3 3H_2O$ was purchased from Himedia and was used without further purification. The starting complexes $[RuCl_3(PPh_3)_3]$,[39] $[RuCl_3(AsPh_3)_3]$,[40] $[RuBr_3(AsPh_3)_3]$[41] and the Schiff bases[42] were prepared by reported literature methods.

Preparation of ruthenium (III) complexes

The new complexes were prepared by the following general procedure. To a solution of $[RuX_3(EPh_3)_3]$ (X = Cl or Br, E = P or As; 0.099–0.125 g, 0.1 mmol) in benzene (20 cm^3), the appropriate Schiff base ligand (0.021–0.032 g, 0.1 mmol) was added and the mixture was heated under reflux for 6 h. The resulting solution was concentrated to *ca* 3 cm^3 and cooled, and the product was separated by the addition of a small amount of light petroleum (60–80 °C). The product was filtered and recrystallized from CH_2Cl_2–light petroleum (60–80 °C) mixture and dried *in vacuo* (yield 70–85%).

Methods

The analyses of carbon, hydrogen, nitrogen and sulfur were performed on Carlo Erba 1106 and Perkin-Elmer model 240 CHN analysers at the Central drug research institute, Lucknow, India. IR spectra were recorded in KBr pellets with Shimadzu/Nicolet instruments in the 4000–400 cm^{-1} range. The EPR spectra of powdered samples were recorded at 298 and 77 K with Jeol Tel-100 at X-band frequencies using DPPH (2,2′-Diphenyl-1-picrylhydrazine hydrate) as internal standard. Magnetic susceptibility measurements of the complexes were made on an EG and G-PARC vibrating sample magnetometer. Cyclic voltammetric studies were carried out on an EG&G Princeton Applied Research Electrochemical Analyser, in acetonitrile using a glassy-carbon working electrode and the potentials were referenced to a silver–silver chloride electrode. Melting points were recorded with a Raaga apparatus and are uncorrected.

The transmission mode EXAFS measurements were performed at Ru K-edge at 22 117 eV with Si(311) double crystal monochromator at the beamline X1.1 and at As K-edge at 11 867 eV with Si(111) double crystal monochromator at the beamline A1, at the Hamburger Synchrotron Radiation Laboratory (HASYLAB), Hamburg. Measurements were carried out under ambient conditions and ion chambers filled with inert gases (nitrogen, argon or krypton) were used to measure the incident and transmitted intensities. The positron energy was 4.45 GeV and the beam current was between 90 and 130 mA. The complexes in solid state were embedded in a polyethylene matrix and pressed into pellets, and the concentration was adjusted to yield an extinction of 1.5. The data were analysed with a program package especially developed for the requirements of amorphous samples.[43] The program WINXAS[44] was used for normalization, AUTOBK[45] was used for the removal of background and EXCURV98[46] was used for the evaluation of EXAFS function. Curved wave theory with XALPHA phase and amplitude functions was used for the data analysis in *k* space and the resulting EXAFS function was weighted with k^3. The mean free paths of the scattered electrons were calculated from the imaginary part of the potential (VPI set to −4.00), the amplitude reduction factor AFAC was fixed at 0.8 and a Fermi energy shift E_F was introduced to give a best fit to the data.

Catalytic oxidation of benzyl alcohol and cyclohexanol

To a solution of alcohol (1 mmol) in CH_2Cl_2 (20 cm^3), *N*-methyl morpholine-*N*-oxide (NMO; 3 mmol) and the ruthenium complex (0.01 mmol) were added. The solution was stirred for 3 h at room temperature and the mixture was evaporated to dryness and extracted with petroleum ether (60–80 °C). The petroleum ether extract was evaporated to give the corresponding aldehyde/ketone which was then quantified as 2,4-dinitrophenyl hydrazone derivative.[38]

Antibacterial activity

Pathogenic microbials namely *Escherichia coli* and *Pseudomonas* sp. were used to test the biological potential of the thiosemicarbazones and their ruthenium (III) complexes. The antibacterial activity of the compounds was determined by disc diffusion method.[47] The bacteria were cultured in nutrient agar medium in Petri plates and used as inocula for the study. The compounds to be tested were dissolved in DMSO to a final concentration of 0.5 and 1% and soaked in filter paper discs of 5 mm diameter and 1 mm thickness. These discs were placed on the previously seeded plates and incubated at $35 \pm 2\,^{\circ}C$ for 24 h. The diameter (mm) of the inhibitory zone around each disc was measured after 24 h. *Streptomycin* was used as standard.

RESULTS AND DISCUSSION

Preparation of ruthenium (III) complexes

New hexa-coordinated light- and air-stable ruthenium (III) complexes of the type $[RuX(EPh_3)_2(L)]$ (X = Cl or Br; E = As or P; L = tridentate dianionic Schiff base) have been prepared by reacting $[RuX_3(EPh_3)_3]$ with the respective Schiff base in a 1 : 1 molar ratio in benzene.

$$[RuX_3(EPh_3)_3] + H_2L \xrightarrow[\text{Reflux, 6 h}]{\text{Benzene}} [RuX(EPh_3)_2(L)] + 2HX + EPh_3$$

All the new complexes are soluble in most of the common organic solvents. Analytical data for the new complexes (Table 1) agree very well with proposed molecular formulae.

IR studies

The free Schiff bases show a very strong absorption around 1600–1620 cm^{-1} in the IR spectra which is characteristic of the azomethine ν(C═N) group. In the IR spectra of the new complexes the absorption due to >C═N is observed at a lower region (1595–1612 cm^{-1}), indicating the coordination through the azomethine nitrogen.[47] Another medium intensity band, at 3300 cm^{-1} in the free ligands due to ν(OH), was absent in the complexes, indicating deprotonation of the Schiff bases prior to the coordination through the phenolic oxygen atom.[48] This is further supported by the increase in the absorption frequency of phenolic C–O band from 1263–1270 cm^{-1} in the free ligands to 1315–1340 cm^{-1} in the ruthenium complexes, indicating that the other coordination site of Schiff bases is phenolic oxygen in all the complexes.[35,48] The band of medium intensity at 792–817 cm^{-1} in the spectra of all the ligands may be assigned to the >C═S stretching vibration. This band disappeared in the complexes and a new band appears at 736–744 cm^{-1}. These observations may be attributed to the enolization of the –NH–C═S group and subsequent coordination through the deprotonated sulfur.[49–51] Thus, in all these complexes the Schiff bases behave as dibasic tridentate ligands. In addition, the other characteristic bands due to triphenylphosphine/triphenylarsine were also present in the expected region (Table 2).

EPR studies

The room temperature and liquid nitrogen temperature EPR spectra of powder samples were recorded at X-band frequencies and the spectral data are given in Table 3. The EPR spectra of ruthenium (III) complexes in liquid nitrogen temperature showed no indication of any hyperfine interaction of nuclei with magnetic moments viz. Ru, As, P, Cl and Br. The complexes $[RuCl(PPh_3)_2$(Nap-Nptsc)], $[RuCl(AsPh_3)_2$(Sal-Nptsc)], $[RuCl(AsPh_3)_2$(Sal-Nmtsc)], $[RuBr(AsPh_3)_2$(Sal-Nmtsc)], $[RuBr(AsPh_3)_2$(Nap-Nptsc)] and $[RuBr(AsPh_3)_2$(Nap-Nmtsc)] exhibited three lines with different g values, indicating the presence of magnetic anisotropy (Fig. 2). These values correspond to those obtained for similar ruthenium (III) complexes.[52,53] The presence of three g values is indicative of a rhombic distortion in these

Table 1. Analytical data of ruthenium (III) Schiff base complexes

Complex	m.p (°C)	Elemental analysis calculated (found), %			
		C	H	N	S
$[RuCl(PPh_3)_2$(Sal-Nptsc)]	192	64.45 (63.98)	4.43 (4.25)	4.51 (4.28)	3.45 (3.44)
$[RuCl(PPh_3)_2$(Sal-Nmtsc)]	183	62.24 (61.94)	4.52 (4.92)	4.84 (5.18)	3.69 (4.01)
$[RuCl(PPh_3)_2$(Nap-Nptsc)]	154	66.28 (65.14)	4.22 (4.34)	4.29 (4.16)	3.27 (4.18)
$[RuCl(PPh_3)_2$(Nap-Nmtsc)]	163	64.23 (65.62)	4.28 (4.67)	4.58 (4.32)	3.50 (4.24)
$[RuCl(AsPh_3)_2$(Sal-Nptsc)]	171	58.98 (60.14)	4.05 (3.24)	4.14 (3.82)	3.15 (3.68)
$[RuCl(AsPh_3)_2$(Sal-Nmtsc)]	138	56.52 (55.86)	4.11 (4.28)	4.39 (4.63)	3.35 (4.06)
$[RuCl(AsPh_3)_2$(Nap-Nptsc)]	149	60.82 (61.24)	3.87 (3.64)	3.94 (4.67)	3.00 (3.92)
$[RuCl(AsPh_3)_2$(Nap-Nmtsc)]	199	56.12 (55.98)	3.91 (3.87)	4.18 (4.86)	3.19 (3.76)
$[RuBr(AsPh_3)_2$(Sal-Nptsc)]	145	56.56 (56.40)	3.95 (3.88)	3.95 (3.88)	3.02 (2.99)
$[RuBr(AsPh_3)_2$(Sal-Nmtsc)]	158	54.01 (53.90)	3.92 (3.80)	4.20 (4.10)	3.20 (3.15)
$[RuBr(AsPh_3)_2$(Nap-Nptsc)]	181	58.39 (59.14)	3.72 (3.84)	3.78 (4.06)	2.88 (3.64)
$[RuBr(AsPh_3)_2$(Nap-Nmtsc)]	240	56.12 (56.96)	3.74 (4.15)	4.01 (4.98)	3.06 (3.81)

complexes. The complexes [RuCl(PPh$_3$)$_2$(Sal-Nptsc)], and [RuCl(PPh$_3$)$_2$(Sal-Nmtsc)] exhibited the spectra with $g_\perp$ at 2.51 and 2.53, and $g_\parallel$ at 2.20 and 2.26. The two different g values ($g_x = g_y \neq g_z$) are indicative of a tetragonal distortion in these octahedral complexes.[54] The presence of two g values also indicates an axial symmetry for these complexes and hence, the *trans* positions are assigned for triphenylphosphine/triphenylarsine groups.[55] Moreover, two of the complexes, [RuCl(AsPh$_3$)$_2$(Nap-Nmtsc)] and [RuCl(PPh$_3$)$_2$(Nap-Nmtsc)], exhibit a single isotropic resonance with g values in the 2.08–2.14 range, indicating a very high symmetry around the ruthenium ions. Such isotropic lines are usually observed either due to the intermolecular spin exchange which can broaden the lines or due to occupancy of the unpaired electrons in a degenerate orbital. There

Table 2. IR spectral data of ruthenium (III) complexes

Complex	$\nu_{(C=N)}$ (cm^{-1})	$\nu_{(C-O)}$ (cm^{-1})	$\nu_{(C-S)}$ (cm^{-1})	Bands due to PPh$_3$/AsPh$_3$
[RuCl(PPh$_3$)$_2$ (Sal-Nptsc)]	1595	1313	737	1436, 1086, 690
[RuCl(PPh$_3$)$_2$ (Sal-Nmtsc)]	1602	1325	736	1411, 1075, 690
[RuCl(PPh$_3$)$_2$ (Nap-Nptsc)]	1597	1329	739	1439, 1060, 689
[RuCl(PPh$_3$)$_2$ (Nap-Nmtsc)]	1600	1336	738	1435, 1076, 692
[RuCl(AsPh$_3$)$_2$ (Sal-Nptsc)]	1595	1325	744	1435, 1092, 692
[RuCl(AsPh$_3$)$_2$ (Sal-Nmtsc)]	1600	1325	744	1435, 1091, 692
[RuCl(AsPh$_3$)$_2$ (Nap-Nptsc)]	1596	1320	742	1435, 1092, 692
[RuCl(AsPh$_3$)$_2$ (Nap-Nmtsc)]	1600	1330	744	1435, 1092, 692
[RuBr(AsPh$_3$)$_2$ (Sal-Nptsc)]	1596	1320	738	1435, 1082, 694
[RuBr(AsPh$_3$)$_2$ (Sal-Nmtsc)]	1612	1340	738	1437, 1060, 692
[RuBr(AsPh$_3$)$_2$ (Nap-Nptsc)]	1597	1332	738	1425, 1060, 690
[RuBr(AsPh$_3$)$_2$ (Nap-Nmtsc)]	1608	1320	738	1458, 1096, 692

Table 3. EPR spectral data of ruthenium (III) complexes

Complex	Temperature (K)	g_x	g_y	g_z	$< g >$
[RuCl(PPh$_3$)$_2$ (Sal-Nptsc)]	77	2.53	2.53	2.20	2.369
[RuCl(PPh$_3$)$_2$ (Sal-Nmtsc)]	298	2.51	2.51	2.26	2.38
[RuCl(PPh$_3$)$_2$ (Nap-Nptsc)]	298	2.51	2.19	2.10	2.28
	77	2.50	2.19	2.10	2.27
[RuCl(PPh$_3$)$_2$ (Nap-Nmtsc)]	298	2.14	2.14	2.14	2.14
[RuCl(AsPh$_3$)$_2$ (Sal-Nptsc)]	298	2.89	2.39	2.22	2.51
	77	2.38	2.23	2.02	2.22
[RuCl(AsPh$_3$)$_2$ (Sal-Nmtsc)]	298	2.93	2.43	2.20	2.54
[RuCl(AsPh$_3$)$_2$ (Nap-Nmtsc)]	298	2.08	2.08	2.08	2.08
	77	2.09	2.09	2.09	2.09
[RuBr(AsPh$_3$)$_2$ (Sal-Nmtsc)]	298	2.45	2.21	2.12	2.26
	77	2.44	2.20	2.11	2.25
[RuBr(AsPh$_3$)$_2$ (Nap-Nptsc)]	298	2.42	2.23	2.12	2.26
	77	2.42	2.23	2.10	2.25
[RuBr(AsPh$_3$)$_2$ (Nap-Nmtsc)]	298	2.43	2.18	2.09	2.24
	77	2.44	2.20	2.10	2.25

$< g >^* = [1/3\, g_x^2 + 1/3\, g_y^2 + 1/3\, g_z^2]^{1/2}$

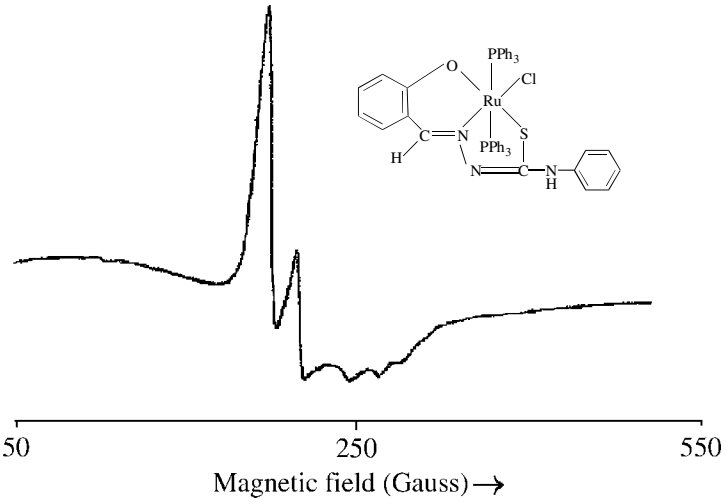

Figure 2. EPR spectrum of [RuCl(PPh$_3$)$_2$(Sal-Nptsc)] at 77 K.

exists no significant variation in the EPR spectra of the complexes recorded at room temperature and liquid nitrogen temperature. In addition, the nature and position of the lines in the spectra of these complexes are similar to those of the other octahedral complexes.[56]

Electrochemical studies

Cyclic voltammetric studies have been carried out for the ruthenium (III) Schiff base complexes in acetonitrile solution using a glassy carbon working electrode. All potentials were referenced to silver–silver chloride electrode. The cyclic voltammetric data are given in Table 4 and a representative case is displayed in Fig. 3. As the ligands used in this work are not reversibly reduced within the potential limit (0 to −2 V), we believe that the reduction process observed for these complexes are metal-centered only. All the complexes showed only a reversible reduction wave in the −0.7 to −1.15 V range. The high peak-to-peak separation value (ΔE_p = 210–420 mV) reveals that this process is quasi-reversible.[57] This is attributed to slow electron transfer and adsorption of the complexes onto the electrode surface.[58] The ruthenium (III) to ruthenium (II) redox processes are influenced by the coordination number, stereochemistry and the hard/soft character of the ligands donor atoms. However, owing to inherent difficulties in relating coordination number and stereochemistry of the species present in solution, redox processes are generally described in terms of the nature of the ligands present.[59] Patterson and Holm[60] have shown that softer ligands tend to produce more positive E_o values, while hard acids give rise to negative E_o values. The observed E_o values for the thiosemicarbazone complexes indicate considerable hard acid character, which is likely to be due to an azomethine nitrogen donor atom involved in the coordination. It has also been observed that little variation exists in the redox potentials due to replacement of PPh_3 or $AsPh_3$ and also to the nature of the ligand. A similar behaviour has been observed for other ruthenium (III) complexes as well.[61]

Table 4. Cyclic voltammetric data of ruthenium (III) complexes

Complex	E_{pa}	E_{pc}	E_f	ΔE_p
[RuCl(PPh_3)$_2$(Sal-Nptsc)]	−0.76	−0.99	−0.875	230
[RuCl(PPh_3)$_2$(Sal-Nmtsc)]	−0.75	−0.99	−0.87	240
[RuCl(PPh_3)$_2$(Nap-Nptsc)]	−0.70	−0.91	−0.805	210
[RuCl(PPh_3)$_2$(Nap-Nmtsc)]	−0.73	−1.05	−0.89	320
[RuCl($AsPh_3$)$_2$(Sal-Nptsc)]	−0.91	−1.15	−1.03	240
[RuCl($AsPh_3$)$_2$(Sal-Nmtsc)]	−0.81	−1.03	−0.92	220
[RuCl($AsPh_3$)$_2$(Nap-Nptsc)]	−0.82	−1.12	−0.97	300
[RuCl($AsPh_3$)$_2$(Nap-Nmtsc)]	−0.77	−0.98	−0.875	210
[RuBr($AsPh_3$)$_2$(Sal-Nptsc)]	−0.81	−1.05	−0.93	240
[RuBr($AsPh_3$)$_2$(Sal-Nmtsc)]	−0.78	−1.2	−0.99	420
[RuBr($AsPh_3$)$_2$(Nap-Nptsc)]	−0.85	−1.08	−0.965	230
[RuBr($AsPh_3$)$_2$(Nap-Nmtsc)]	−0.80	−1.04	−0.92	240

Supporting electrolyte: $[NBu_4]BF_4$ (0.1 M); concentration of the complex: 0.001 M; scan rate: 100 mV s^{-1}; all the potentials are referenced to Ag–AgCl; $E_f = 0.5\ (E_{pa} + E_{pc})$, where E_{pa} and E_{pc} are anodic and cathodic potentials, respectively.

EXAFS studies

Despite several attempts, single crystals suitable for X-ray structure determination could not be obtained. Hence, the local structure and the coordination geometry of the complexes were determined by EXAFS spectroscopy, which is a powerful technique for probing the neighbourhood environment of a selected atom regardless of the physical state of the sample. EXAFS provides information on the coordination number, the nature of the scattering atoms surrounding the absorbing atom, the interatomic distance between the absorbing atom and the backscattering atoms and the Debye–Waller factor, which accounts for the disorders due to the static displacements and thermal vibrations.[62,63] EXAFS studies were performed on selected five complexes at the Ru and As K-edges. In the fitting procedure, for all the complexes the coordination numbers were fixed to known values for different backscatterers surrounding the excited atom, and the other parameters, including interatomic

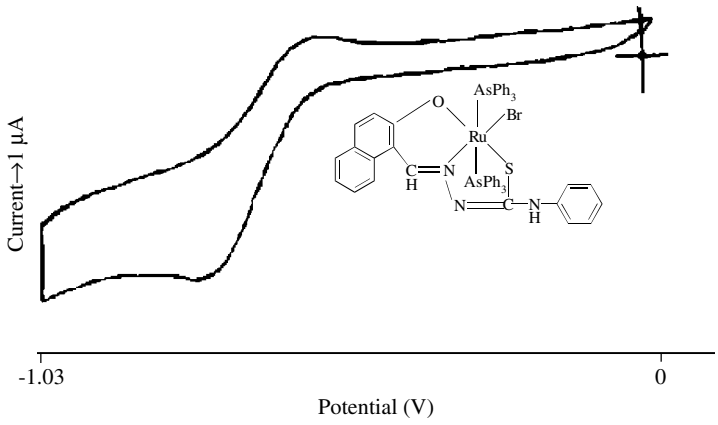

Figure 3. Cyclic voltammogram of [RuBr($AsPh_3$)$_2$(Nap-Nptsc)].

distances, Debye–Waller factor and Fermi energy value, were varied by iterations.

Ru K-edge investigations

The experimentally determined and theoretically calculated EXAFS functions in *k* space and their Fourier transforms in real space for the different ruthenium (III) complexes measured at the Ru K-edge are shown in Fig. 4 and the corresponding structural parameters are summarized in Table 5. In the analyses of the complexes, the first shell was fitted with a coordination number of two consisting of a nitrogen and an oxygen backscatterer from the coordinating ligand, at about 2.06 Å in the case of arsenic containing complexes ([RuCl($AsPh_3$)$_2$(Sal-Nptsc)], [RuCl($AsPh_3$)$_2$(Nap-Nptsc)] and [RuCl($AsPh_3$)$_2$(Nap-Nmtsc)]), at about 2.04 Å in the case of [RuCl(PPh_3)$_2$(Nap-Nptsc)] and at 2.01 Å in the case of [RuCl(PPh_3)$_2$(Nap-Nmtsc)]. Owing to the similar backscattering behaviour of the near neighbours (nitrogen and oxygen) occurring at nearly the same distance, they could not be fitted separately and thus were fitted as one shell with nitrogen amplitude and phase functions. The observed ruthenium–nitrogen and ruthenium–oxygen distances are in agreement with those of analogous ruthenium complexes.[64,65] The second shell was determined at about 2.35 Å distance in all the complexes. In [RuCl($AsPh_3$)$_2$(Sal-Nptsc)], [RuCl($AsPh_3$)$_2$(Nap-Nptsc)] and [RuCl($AsPh_3$)$_2$(Nap-Nmtsc)], the second shell consisted of one sulfur and one chlorine backscatterers, whereas in [RuCl(PPh_3)$_2$(Nap-Nptsc)] and [RuCl(PPh_3)$_2$(Nap-Nmtsc)], the second shell consisted of one sulfur, two phosphorus and one chlorine backscatterers. For the same reason as stated earlier, a single shell was fitted with the combined coordination number, with sulfur amplitude and phase functions. For comparison, the reported ruthenium–sulfur distances ranges from 2.23 to 2.37 Å in *fac*-[Ru($C_6H_5NHC_4O_3$)(Cl)(*dmso*)$_3$(H_2O]·3H_2O,[66] ruthenium–phosphorus distances ranges from 2.32 to 2.37 Å in *cis*-[Ru(*dppm*)$_2$($MeCN$)$_2$]-(BF_4)$_2$[64] and ruthenium–chlorine distances ranges from 2.35 to 2.39 Å

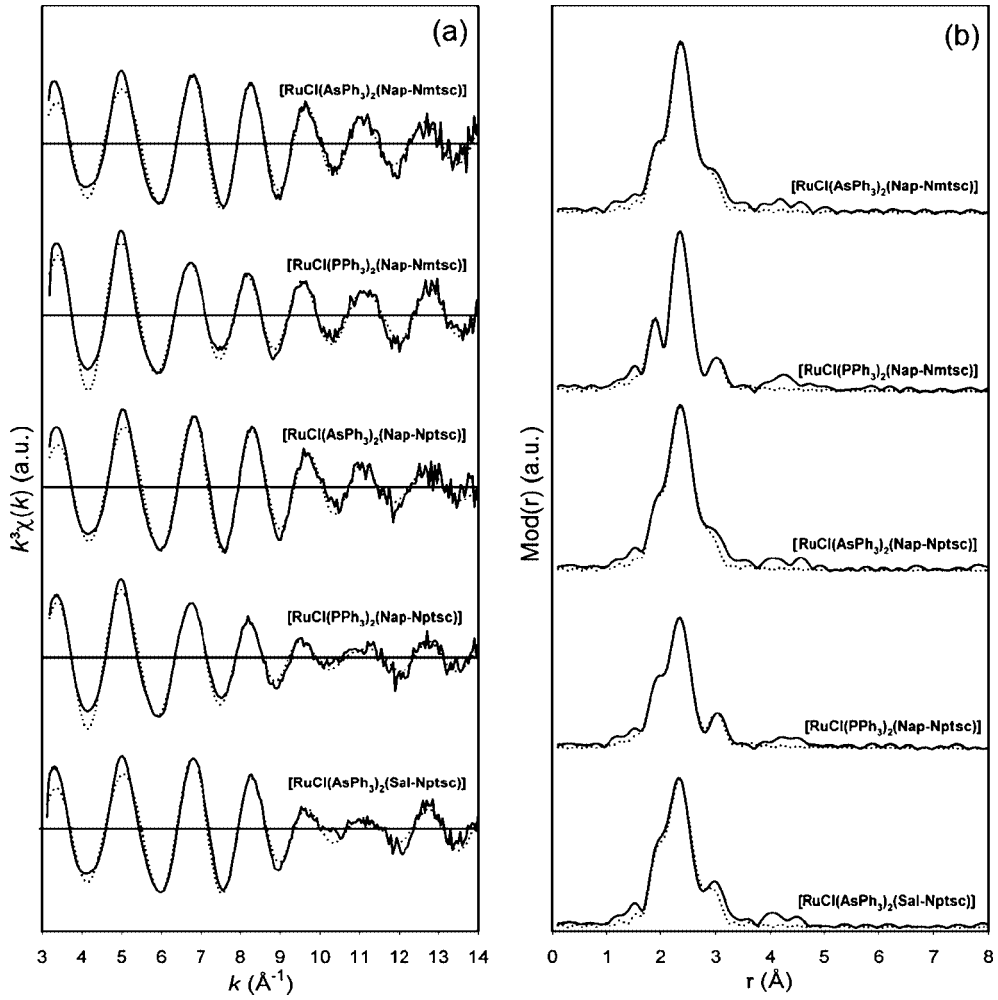

Figure 4. Experimental (solid line) and calculated (dotted line) EXAFS functions and their corresponding Fourier transform plots for the different ruthenium (III) complexes measured at the Ru K-edge.

Table 5. EXAFS determined structural parameters at Ru K-edge

Complex	A–Bs[a]	N[b]	r[c] [Å]	σ[d] [Å]	E_F[e] (eV)	k-range (Å^{-1})	R-factor
[RuCl(AsPh$_3$)$_2$(Sal-Nptsc)]	Ru-N/O	2	2.06 ± 0.02	0.050 ± 0.005	4.682	3.13–14.04	22.83
	Ru-S/Cl	2	2.35 ± 0.03	0.063 ± 0.009			
	Ru-As	2	2.55 ± 0.04	0.120 ± 0.018			
	Ru-C	3	2.96 ± 0.05	0.071 ± 0.014			
[RuCl(PPh$_3$)$_2$(Nap-Nptsc)]	Ru-N/O	2	2.04 ± 0.02	0.067 ± 0.007	5.584	3.20–14.05	20.23
	Ru-S/P/Cl	4	2.36 ± 0.03	0.095 ± 0.014			
	Ru-C	3	2.99 ± 0.05	0.059 ± 0.012			
[RuCl(AsPh$_3$)$_2$(Nap-Nptsc)]	Ru-N/O	2	2.05 ± 0.02	0.059 ± 0.006	5.531	3.19–14.05	22.69
	Ru-S/Cl	2	2.34 ± 0.03	0.067 ± 0.010			
	Ru-As	2	2.53 ± 0.04	0.102 ± 0.015			
	Ru-C	3	2.91 ± 0.05	0.081 ± 0.016			
[RuCl(PPh$_3$)$_2$(Nap-Nmtsc)]	Ru-N/O	2	2.01 ± 0.02	0.059 ± 0.006	6.352	3.20–14.01	20.12
	Ru-S/P/Cl	4	2.37 ± 0.03	0.084 ± 0.013			
	Ru-C	3	2.98 ± 0.05	0.063 ± 0.013			
[RuCl(AsPh$_3$)$_2$(Nap-Nmtsc)]	Ru-N/O	2	2.06 ± 0.02	0.059 ± 0.006	5.036	3.17–14.05	21.45
	Ru-S/Cl	2	2.36 ± 0.03	0.063 ± 0.009			
	Ru-As	2	2.52 ± 0.04	0.107 ± 0.016			
	Ru-C	3	2.93 ± 0.05	0.067 ± 0.013			

[a] Absorber (A)–backscatterers (Bs); [b] coordination number N; [c] interatomic distance r; [d] Debye–Waller factor σ with its calculated deviation; and [e] Fermi energy E_F.

in *mer*-[RuCl$_3$(AsMe$_2$Ph)$_3$].[67] Additionally, in complexes [RuCl(AsPh$_3$)$_2$(Sal-Nptsc)], [RuCl(AsPh$_3$)$_2$(Nap-Nptsc)] and [RuCl(AsPh$_3$)$_2$(Nap-Nmtsc)], two arsenic backscatterers were determined at about 2.53 Å distance. The determined ruthenium–arsenic distances were in good agreement with those reported for similar organo-ruthenium complexes.[67] Further, in all the complexes, an additional shell consisting of three carbon backscatterers, possibly originating from the proximal carbon atoms of the ligand, could be determined at about 2.98 Å distance (slightly shortened in the case of [RuCl(AsPh$_3$)$_2$(Nap-Nptsc)] and [RuCl(AsPh$_3$)$_2$(Nap-Nmtsc)]). The obtained EXAFS results indicate 6-fold coordination geometry around the ruthenium atom.

As K-edge investigations

The experimentally determined and theoretically calculated EXAFS functions in k space and their Fourier transforms in real space for the different ruthenium (III) complexes measured at the As K-edge are shown in Fig. 5 and the corresponding structural parameters are summarized in Table 6. In the three investigated complexes, the k^3-weighted EXAFS function could best be described by a three-shell model. The first shell at about 1.93 Å distance was fitted with three carbon backscatterers originating from the three proximal carbon atoms of the coordinating triphenyl group, the second shell consisting of a single ruthenium backscatterer was determined at about 2.49 Å and the third shell comprising six carbon backscatterers stemming from the second near-neighbour carbon atoms of the phenyl ring was determined at about 2.91 Å distance. The reported arsenic–carbon distances ranges from 1.90 to 1.97 Å and arsenic–ruthenium distances ranges from 2.46 to 2.51 Å, in *mer*-[RuCl$_3$(AsMe$_2$Ph)$_3$] and *mer*-[RuBr$_3$(AsMe$_2$Ph)$_3$].[67] In all the complexes, the arsenic–ruthenium distances determined from the As K-edge measurements were slightly shorter than those determined from the Ru K-edge measurements. In addition, in all the cases, the fitting of the EXAFS function to the experimental spectra resulted in very high R-factor values. This could be attributed to the ambiguous coordination geometry around the arsenic atom and apart from the first three shells; the other shells could not be fitted unequivocally. Furthermore, to confirm this supposition, Fourier filter analysis was performed in the range 1.0–3.0 Å, in order that the contributions from only the first three shells are considered. The experimentally determined and theoretically calculated EXAFS functions in k space and their Fourier transforms in real space for the above-mentioned complexes are shown in Fig. 6 and the results of the Fourier filter analysis are summarized in Table 6. It should be noted that the R-factor value improves considerably by about 38% in the case of [RuCl(AsPh$_3$)$_2$(Sal-Nptsc)], about 37% in the case of [RuCl(AsPh$_3$)$_2$(Nap-Nptsc)] and about 39% in the case of [RuCl(AsPh$_3$)$_2$(Nap-Nmtsc)].

Magnetic moments

The magnetic moments for some of the complexes have been measured at room temperature using a vibrating sample magnetometer. The values lie between 1.70 and 2.10, indicating the presence of one unpaired electron and +3 oxidation state for ruthenium in all these complexes.[68]

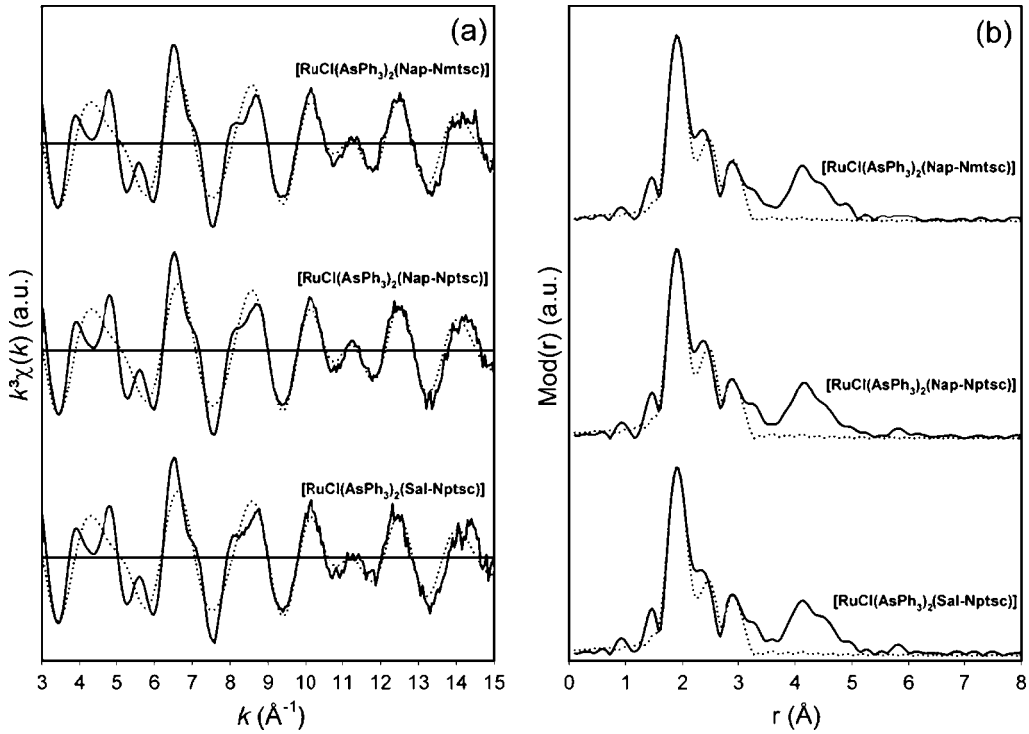

Figure 5. Experimental (solid line) and calculated (dotted line) EXAFS functions and their corresponding Fourier transform plots for the different ruthenium (III) complexes measured at the As K-edge.

Table 6. EXAFS determined structural parameters at As K-edge

Complex	A–Bs[a]	N[b]	r[c] (Å)	σ[d] (Å)	E_F[e] (eV)	k-range (Å^{-1})	R-factor
[RuCl(AsPh$_3$)$_2$(Sal-Nptsc)]	As-C	3	1.94 ± 0.02	0.050 ± 0.005	−3.654	3.00–15.04	45.73
	As-Ru	1	2.49 ± 0.04	0.089 ± 0.013			
	As-C	6	2.91 ± 0.05	0.077 ± 0.015			
[RuCl(AsPh$_3$)$_2$Nap-Nptsc)]	As-C	3	1.93 ± 0.02	0.050 ± 0.005	−3.130	3.02–15.05	41.24
	As-Ru	1	2.49 ± 0.04	0.084 ± 0.013			
	As-C	6	2.91 ± 0.05	0.074 ± 0.015			
[RuCl(AsPh$_3$)$_2$(Nap-Nmtsc)]	As-C	3	1.94 ± 0.02	0.050 ± 0.005	−3.663	3.00–15.04	42.15
	As-Ru	1	2.49 ± 0.04	0.087 ± 0.013			
	As-C	6	2.91 ± 0.05	0.074 ± 0.015			
[RuCl(AsPh$_3$)$_2$(Sal-Nptsc)][f]	As-C	3	1.93 ± 0.02	0.050 ± 0.005	−1.858	3.10–15.06	28.15
	As-Ru	1	2.49 ± 0.04	0.089 ± 0.013			
	As-C	6	2.90 ± 0.05	0.074 ± 0.015			
[RuCl(AsPh$_3$)$_2$(Nap-Nptsc)][f]	As-C	3	1.93 ± 0.02	0.050 ± 0.005	−1.569	3.09–15.06	25.81
	As-Ru	1	2.49 ± 0.04	0.084 ± 0.013			
	As-C	6	2.90 ± 0.05	0.074 ± 0.015			
[RuCl(AsPh$_3$)$_2$(Nap-Nmtsc)][f]	As-C	3	1.93 ± 0.02	0.050 ± 0.005	−1.435	3.12–15.06	25.75
	As-Ru	1	2.49 ± 0.04	0.087 ± 0.013			
	As-C	6	2.90 ± 0.05	0.074 ± 0.015			

[a] Absorber (A)–backscatterers (Bs); [b] coordination number N; [c] interatomic distance r; [d] Debye–Waller factor σ with its calculated deviation; and [e] Fermi energy E_F. [f] Evaluated using Fourier filter analysis (1.0–3.0 Å range).

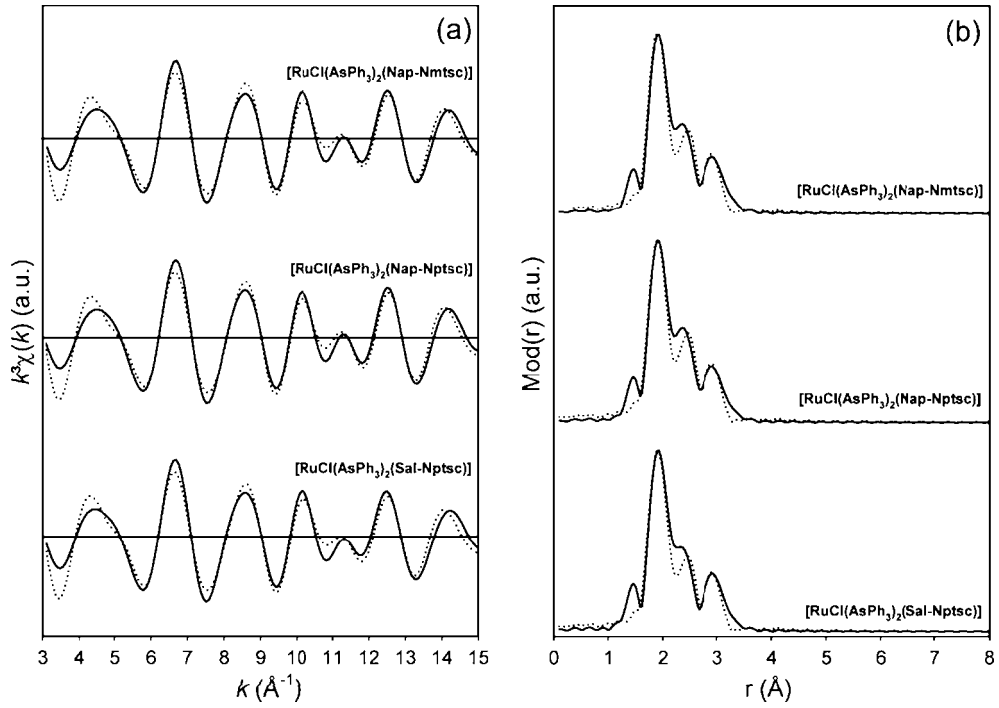

Figure 6. Experimental (solid line) and calculated (dotted line) EXAFS functions and their corresponding Fourier transform plots for the different ruthenium (III) complexes measured at the As K-edge evaluated using Fourier filter analysis (1.0–3.0 Å range).

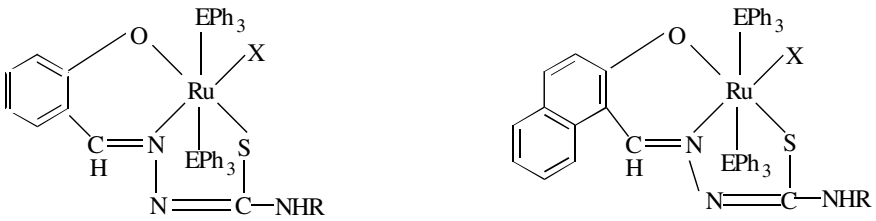

R = C_6H_5, CH_3

$EPh_3 = PPh_3$, $AsPh_3$

X= Br or Cl

[$RuCl(PPh_3)_2$(Sal-Nptsc)] - R = C_6H_5, E = P, X = Cl
[$RuCl(PPh_3)_2$(Sal-Nmtsc)] - R = CH_3, E = P, X = Cl
[$RuCl(AsPh_3)_2$(Sal-Nptsc)] - R = C_6H_5, E = As, X = Cl
[$RuCl(AsPh_3)_2$(Sal-Nmtsc)] - R = CH_3, E = As, X = Cl
[$RuBr(AsPh_3)_2$(Sal-Nptsc)] - R = C_6H_5, E = As, X = Br
[$RuBr(AsPh_3)_2$(Sal-Nmtsc)] - R = CH_3, E = As, X = Br

[$RuCl(PPh_3)_2$(Nap-Nptsc)] - R = C_6H_5, E = P, X = Cl
[$RuCl(PPh_3)_2$(Nap-Nmtsc)] - R = CH_3, E = P, X = Cl
[$RuCl(AsPh_3)_2$(Nap-Nptsc)] - R = C_6H_5, E = As, X = Cl
[$RuCl(AsPh_3)_2$(Nap-Nmtsc)] - R = CH_3, E = As, X = Cl
[$RuBr(AsPh_3)_2$(Nap-Nptsc)] - R = C_6H_5, E = As, X = Br
[$RuBr(AsPh_3)_2$(Nap-Nmtsc)] - R = CH_3, E = As, X = Br

Figure 7. Structure of the ruthenium (III) complexes.

Based on the elemental analysis, IR, EPR, EXAFS and electrochemical studies, an octahedral structure (Fig. 7) has been confirmed for the new ruthenium (III) Schiff base complexes.

Catalytic studies

The oxidation of benzyl alcohol and cyclohexanol using the different ruthenium complexes as catalysts in the presence of *N*-methylmorpholine-*N*-oxide (NMO) as co-oxidant were carried out in dichloromethane. The results of the catalytic oxidation by ruthenium (III) complexes are summarized in Table 7. Benzaldehyde was formed from benzyl alcohol and cyclohexanol was converted into cyclohexanone after 3 h of stirring at room temperature. The aldehyde/ketone formed were quantified as their 2,4-dinitrophenylhydrazone derivatives. In no case was there any detectable oxidation of alcohols in the presence of *N*-methylmorpholine-*N*-oxide alone without the ruthenium complexes. All the synthesized ruthenium complexes were found to catalyse the oxidation of alcohols to aldehydes/ketones, but the yields and the

Table 7. Catalytic oxidation of alcohol by ruthenium (III) Schiff base complexes

Complex	Substrate	Product[a]	Yield[b]	Turn-over[c]
$RuCl(PPh_3)_2$ (Sal-Nptsc)	Benzyl alcohol	A	60.82	61.33
	Cyclohexanol	K	31.33	31.59
$RuCl(PPh_3)_2$ (Sal-Nmtsc)	Benzyl alcohol	A	53.13	53.57
	Cyclohexanol	K	27.99	28.23
$RuCl(PPh_3)_2$ (Nap-Nptsc)	Benzyl alcohol	A	67.61	68.17
	Cyclohexanol	K	33.50	33.78
$RuCl(PPh_3)_2$ (Nap-Nmtsc)	Benzyl alcohol	A	54.10	54.55
	Cyclohexanol	K	28.45	28.69
$RuCl(AsPh_3)_2$ (Sal-Nptsc)	Benzyl alcohol	A	48.00	48.40
	Cyclohexanol	K	27.50	27.73
$RuCl(AsPh_3)_2$ (Sal-Nmtsc)	Benzyl alcohol	A	51.00	51.43
	Cyclohexanol	K	26.00	26.22

[a] A = benzaldehyde; K = cyclohexanone; [b] yields based on substrate; [c] moles of product per mole or catalyst.

turnover were found to vary with different catalysts. The relatively higher product yield obtained for the oxidation of benzyl alcohol than for cyclohexanol was due to the fact that the α-CH moiety of benzyl alcohol is more acidic than that of cyclohexanol.[68] It has also been found that triphenylphosphine complexes possess higher catalytic activity than the triphenylarsine complexes.[69] This may be due to the higher donor ability of the arsine ligand compared with that of phosphine. It has also been found that ruthenium (III) complexes derived from 4(N) methyl thiosemicarbazone ligands showed less catalytic activity when compared with other complexes, which could be attributed to the presence of the electron-releasing methyl group in these complexes, which decreases the catalytic activity by increasing the electron density on the metal ion.[70]

Antibacterial studies

The *in vitro* antibacterial screening of the ligands and their ruthenium complexes was carried out against *Escherichia coli* and *Pseudomonas* sp. using a nutrient agar medium by disc diffusion method. The results (Table 8) showed that the complexes exhibit moderate activity against *Escherichia coli* and *Pseudomonas* sp. The possible mode of increased toxicity of the ruthenium (III) complexes compared with that of the free ligands may be explained by Tweedy's chelating theory,[71] according to which chelation reduces the polarity of the central metal atom because of partial sharing of its positive charge with the ligand, which favours the permeation of the complexes through the lipid layer of cell membranes. Although the complexes were active, they did not reach the effectiveness of the conventional bactericide, *Streptomycin*.

Table 8. Antibacterial activity of Schiff base ligands and ruthenium (III) complexes

	Diameter of inhibition zones (mm)			
	Escherichia coli		*Pseudomonas* sp.	
Ligand/complex	0.5%	1.0%	0.5%	1.0%
H_2-Sal-Nptsc	10	13	10	12
H_2-Sal-Nmtsc	9	11	10	11
H_2-Nap-Nptsc	9	13	10	12
H_2-Nap-Nmtsc	10	13	10	12
$[RuCl(PPh_3)_2$(Sal-Nptsc)]	12	15	11	13
$[RuCl(PPh_3)_2$(Sal-Nmtsc)]	11	16	12	14
$[RuCl(PPh_3)_2$(Nap-Nptsc)]	11	14	12	15
$[RuCl(PPh_3)_2$(Nap-Nmtsc)]	11	15	12	14
$[RuCl(AsPh_3)_2$(Sal-Nptsc)]	13	14	12	13
$[RuCl(AsPh_3)_2$(Sal-Nmtsc)]	10	12	12	14
$[RuCl(AsPh_3)_2$(Nap-Nptsc)]	14	16	11	15
$[RuCl(AsPh_3)_2$(Nap-Nmtsc)]	13	15	14	15

CONCLUSION

Mononuclear ruthenium (III) complexes of the type $[RuX(EPh_3)_2(L)]$ (X = Cl or Br; L = dibasic tridentate Schiff base ligand; E = P or As) were synthesized. Based on the elemental analysis, IR, EPR, EXAFS and electrochemical studies, an octahedral structure was confirmed for the new complexes. The new complexes showed high catalytic activity in the oxidation of alcohols and also exhibited a considerable amount of antibacterial activity towards microbials.

Acknowledgements

HASYLAB at DESY, Hamburg, Germany is gratefully acknowledged for the kind support for the synchrotron radiation experiments. The Central Drug Research Institute, Lucknow, India is thanked for the support for the analytical studies.

REFERENCES

1. Yamazaki O, Tanaka T, Shimada S, Suzuki Y, Tanaka M. *Syn. Lett.* 2004; **11**: 1921.
2. Stoltz BM. *Chem. Lett.* 2004; **33**: 362.
3. Goldstain AS, Neer RH, Drago RS. *J. Am. Chem. Soc.* 1994; **16**: 2424.
4. Karvembu R, Prabhakaran R, Natarajan K. *Coord. Chem. Rev.* 2005; **249**: 911.
5. Kappler BK, Rupp W, Juhl UM, Endres H, Niebl R, Balzer W. *Inorg. Chem.* 1987; **26**: 4366.
6. Quiroga AG, Ranninger CN. *Coord. Rev.* 1994; **248**: 119.
7. Chandhary A, Bansal N, Gajraj A, Singh RV. *J. Inorg. Biol. Chem.* 2003; **96**: 393.
8. Ligthart GBWL, Meijer RH, Hulshof MP. *Tetrahedron Lett.* 2003; **44**: 1507.
9. Lo CY, Guo H, Lian JJ, Shen FM, Liu RS. *J. Org. Chem.* 2002; **67**: 3930.

10. Danopoulos AA, Winston S, Motherwell WB. *Chem. Commun.* 2002; 1376.
11. Dijksman A, Gonzalez AM, Payeras AM, Arends IWCE, Sheldon RA. *J. Am. Chem. Soc.* 2001; **123**: 6826.
12. Ando T, Kamigaito M, Sawamoto M. *Macromol.* 2000; **33**: 5825.
13. Cogan DA, Liu GC, Kim KJ, Backes BJ, Ellman JA. *J. Am. Chem. Soc.* 1998; **120**: 8011.
14. Liu GC, Cogan DA, Ellman JA. *J. Am. Chem. Soc.* 1997; **119**: 9913.
15. Finch AR, Chin LM, Grill SP, Rose WC, Loomis R, Vasquez KM, Cheng YC, Sartorelli AC. *Biochem. Pharmac.* 2000; **59**: 983.
16. Li J, Zheng LM, King I, Doyle TW, Chen SH. *Curr. Med. Chem.* 2001; **8**: 121.
17. Kasuga NC, Sekino K, Ishikawan M, Honda A, Yokoyama M, Nakano S, Shimada N, Koumo C, Nomiya K. *J. Inorg. Biol. Chem.* 2003; **96**: 298.
18. West PX, Liberta AE, Rajendran KG, Hall IH. *Anticancer Drugs* 1993; **4**: 241.
19. Karvembu R, Natarajan K. *Polyhedron* 2002; **21**: 219.
20. Chatterjee D, Misra A, Roy BC. *J. Mol. Catal.* 2000; **161**: 17.
21. Kim SS, Trushkov I, Sar SK. *Bull. Korean Chem. Soc.* 2002; **23**: 1331.
22. Keresszegi C, Mallat T, Baiker A. *New J. Chem.* 2001; **25**: 1163.
23. Backvall JE, Andreasson U. *Tetrahedron Lett.* 1993; **34**: 5459.
24. Jung HM, Choi JH, Lee SO, Kim YH, Park JH, Park J. *Organometallics* 2002; **21**: 5674.
25. Yang H, Alvarez M, Lugan N, Mathieu R. *Chem. Commun.* 1995; 1721.
26. Menashe N, Salant E, Shvo Y. *J. Organomet. Chem.* 1996; **97**: 574.
27. Shvo Y, Goldberg I, Czerkic D, Reshef D, Stein Z. *Organometallics* 1997; **16**: 133.
28. Ito M, Hirakawa M, Murata K, Ikariya T. *Organometallics* 2001; **20**: 379.
29. Rath RK, Nethaji M, Chakravathy AR. *Polyhedron* 2001; **20**: 2735.
30. Cameron BR, Darkes MC, Baird IR, Skerlj RT, Santucci ZL, Fricker SP. *Inorg. Chem.* 2003; **42**: 4102.
31. Karidi K, Garoufis A, Tsipis A, Hadjiliadis N, den Dulk H, Reedijik J. *J. Chem. Soc., Dalton Trans.* 2005; 1176.
32. Anderberg PI, Harding MM, Luck IJ, Turner P. *Inorg. Chem.* 2001; **41**: 1365.
33. Jayabalakrishnan C, Natarajan K. *Trans. Met. Chem.* 2002; **27**: 75.
34. Karvembu R, Hemalatha S, Prabhakaran R, Natarajan K. *Inorg. Chem. Commun.* 2003; **6**: 486.
35. Karvembu R, Natarajan K. *Polyhedron* 2002; **21**: 1721.
36. Prabhakaran R, Geetha A, Thilagavathi M, Karvembu R, Krishnan V, Bertagnolli H, Natarajan K. *J. Inorg. Biochem.* 2004; **98**: 2131.
37. Jayabalakrishnan C, Karvembu R, Natarajan K. *Synth. React. Inorg. Met. Org. Chem.* 2003; **33**: 1535.
38. Vogel AI. *Textbook of Practical Organic Chemistry*. Longman: London, 1989.
39. Chatt J, Leigh GJ, Mingos DMP, Paske RJ. *J. Chem. Soc. A* 1968; 2636.
40. Poddar RK, Khullar IP, Agarwala U. *J. Inorg. Nucl. Chem. Lett.* 1974; **10**: 221.
41. Natarajan K, Poddar RK, Agarwala U. *J. Inorg. Nucl. Chem.* 1972; **39**: 431.
42. Abo SH, Fetoh E, Eid AE, Abd AE, Kareem E, Wassel MA. *Synth. React. Inorg. Met. Org. Chem.* 2000; **30**: 513.
43. Ertel TS, Bertagnolli H, Hueckmann S, Kolb U, Peter D. *Appl. Spectrosc.* 1992; **46**: 690.
44. Ressler T. *J. Phys. IV* 1997; **C2-7**: 269.
45. Newville M, Livins P, Yakoby Y, Rehr JJ, Stern EA. *Phys. Rev. B* 1993; **47**: 14 126.
46. Gurman SJ, Binstead N, Ross I. *J. Phys. C* 1986; **19**: 1845.
47. Dharmaraj N, Viswanathamurthi P, Natarajan K. *Trans. Met. Chem.* 2001; **26**: 105.
48. Khera B, Sharma AK, Kaushik NK. *Polyhedron* 1983; **2**: 1177.
49. Deepa KP, Aravindakshan KK. *Synth. React. Inorg. Met. Org. Chem.* 2000; **30**: 1601.
50. Khan BT, Zakeeruddin SM. *Trans. Met. Chem.* 1991; **16**: 119.
51. Thakur Y, Narinjha B. *J. Inorg. Nucl. Chem.* 1980; **42**: 449.
52. Daniel Thangadurai T, Natarajan K. *Trans. Met. Chem.* 2000; **25**: 347.
53. Khan MMT, Kureshy RI, Khan NH. *Polyhedron* 1991; **1**: 2559.
54. Harris G. *Theor. Chim. Acta* 1966; **5**: 379.
55. Manoharan PT, Mehrotra PK, Khan MMT, Andal RK. *Inorg. Chem.* 1973; **27**: 601.
56. Karvembu R, Jayabalakrishnan C, Dharmaraj N, Renukadevi SV, Natarajan K. *Trans. Met. Chem.* 2002; **27**: 631.
57. Heinze J. *Angew. Chem. Int. Edn* 1984; **23**: 831.
58. Wallce AW, Murphy J, Peterson JD. *Inorg. Chim. Acta* 1989; **166**: 47.
59. Hathaway BJ. In *Comprehensive Coordination Chemistry*, Vol. 5. Pergaman Press: Oxford, 1987.
60. Patterson GS, Holm RH. *J. Biol. Inorg. Chem.* 1975; **4**: 1257.
61. Daniel Thangadurai T, Natarajan K. *Synth. React. Inorg. Met. Org. Chem.* 2001; **31**: 549.
62. Teo BK. *EXAFS: Basic Principles and Data Analysis*. Springer: Berlin, 1986.
63. Lytle FW, Sayers DE, Stern EA. *Phys. Rev. B* 1975; **11**: 4825.
64. Bickley JF, La Pensée AA, Higgins SJ, Stuart CA. *J. Chem. Soc., Dalton Trans.* 2003; 4663.
65. Man WL, Tang TM, Wong TW, Lau TC, Peng SM, Wong WT. *J. Am. Chem. Soc.* 2004; **126**: 478.
66. Piggot PMT, Hall LA, White AJP, Williams DJ. *Inorg. Chim. Acta* 2004; **357**: 207.
67. Holmes NJ, Genge ARJ, Levason W, Webster M. *J. Chem. Soc. Dalton Trans.* 1997; 2331.
68. Figgis BN. *Introduction to Ligand Field Theory*. Interscience: New York, 1966.
69. Kim JY, Jun MJ, Lee WY. *Polyhedron* 1996; **15**: 3787.
70. Bhattacharya PK. *Proc. Ind. Acad. Sci. (Chem. Sci.)* 1990; **102**: 247.
71. Tweedy BG. *Phytopathology* 1964; **55**: 910.